

Original Research

Uncovering Sex-Related Differences in Skin Macrophage Polarization During Wound Healing in Diabetic Mice

Coco X. Huang¹, Elisha Siwan¹, Callum J. Baker^{1,2}, Zhuoran Wei¹, Diana Shinko³, Helen M. McGuire⁴, Stephen M. Twigg^{1,5}, Danqing Min^{1,5},*

Academic Editor: Paramjit S. Tappia

Submitted: 24 October 2024 Revised: 12 December 2024 Accepted: 20 December 2024 Published: 17 February 2025

Abstract

Background: Chronic wounds, such as diabetes-related foot ulcers, arise from delayed wound healing and create significant health and economic burdens. Macrophages regulate healing by shifting between pro- and anti-inflammatory phenotypes, known as macrophage polarization. Sex and diabetes can impair wound healing, but their influence on macrophage phenotype in skin tissue during wound healing remains unclear, which was investigated in this study using a novel two-sex diabetic mouse model. Methods: Diabetes was induced in male and female C57BL/6J mice using low-dose streptozotocin injections and high-fat diet feeding, with chow-fed mice as controls. After 18 weeks, each mouse received four circular full-thickness dorsal skin wounds. The macrophage phenotypes in wounded skin tissues at Day 0 and Day 10 post-wounding were analyzed using mass cytometry with manual gating and automated computational clustering. Results: Male diabetic mice exhibited more severe hyperglycemia and insulin resistance compared to females. Although diabetic mice did not display delayed wound healing, male mice had a greater proportion of total macrophages than females, especially a higher proportion of pro-inflammatory matrix metalloproteinase-9 (MMP-9)+ macrophages and a lower proportion of anti-inflammatory adiponectin receptor 1 (AdipoR1)+ macrophages in male diabetic mice compared to females, indicating an imbalanced polarization towards a pro-inflammatory phenotype that could result in poorer wound healing. Interestingly, computational clustering identified a new pro-inflammatory, pro-healing phenotype (Ly6C+AdipoR1+CD163-CD206-) more abundant in females than males, suggesting this phenotype may play a role in the transition from the inflammatory to the proliferative stage of wound healing. Conclusions: This study demonstrated a significant sex-based difference in macrophage populations, with male diabetic mice showing a pro-inflammatory bias that may impair wound healing, while a unique pro-inflammatory, pro-healing macrophage population more abundant in females could facilitate recovery. Further research is needed to investigate the role of these newly identified phenotypes in regulating impaired wound healing.

Keywords: rodent; diabetes; skin; wound; monocytes/macrophages; cell surface marker; inflammation

1. Introduction

Diabetes-related foot ulcers (DFUs) frequently arise from delayed wound healing in people with diabetes and present a significant health and economic burden [1]. People with diabetes have a 15–25% lifetime risk of developing DFUs, which can require hospitalization and amputation in severe cases [2,3]. This can negatively impact quality of life and mental health, as well as affect morbidity and mortality [4]. Thus, understanding the pathophysiology of impaired wound healing in diabetes is imperative to develop treatments and preventative measures for DFUs, to ease the burden on individuals with diabetes and the healthcare system

In chronic wounds such as DFUs, there is excessive and prolonged inflammation, which subsequently promotes tissue injury and inhibits wound healing [5]. Macrophages are key mediators of wound healing as they can polarize to express different cellular markers and adopt different functions at various stages of wound healing [6]. Macrophages present in skin are a mixture of tissue-resident macrophages such as epidermal Langerhans cells (CD207+) [7] and infiltrating macrophages from the bloodstream. Generally, macrophages can be classified as M1 (pro-inflammatory) or M2 (anti-inflammatory/pro-healing) [8], but they can switch between phenotypes [6] or exhibit a spectrum of both [9]. Disrupting the M1/M2 balance is known to prolong inflammation and delay wound healing, while interventions that regulate this balance or promote M2 polarization may improve wound healing [10].

Ly6C, a common phenotypic marker, is expressed by murine monocytes and macrophages. Ly6C+ and Ly6C-

¹Greg Brown Diabetes and Endocrine Research Laboratory, Sydney Medical School (Central), Faculty of Medicine and Health, Charles Perkins Centre, The University of Sydney, NSW 2006, Australia

 $^{^2}$ School of Health Sciences, Faculty of Medicine and Health, The University of Sydney, Sydney, NSW 2006, Australia

 $^{^3\}mathrm{Sydney}$ Cytometry, The University of Sydney, Sydney, NSW 2006, Australia

⁴School of Medical Sciences, Faculty of Medicine and Health, Charles Perkins Centre, The University of Sydney, Sydney, NSW 2006, Australia

⁵Department of Endocrinology, Royal Prince Alfred Hospital, Sydney, NSW 2050, Australia

^{*}Correspondence: danqing.min@sydney.edu.au (Danqing Min)

monocytes are analogous to classical (CD14+CD16-) and non-classical (CD14+CD16+) monocytes in humans, which have pro-inflammatory and regenerative functions respectively [11]. A diabetic mouse model [12] demonstrated the increased recruitment and predominance of Ly6C+ macrophages during later stages of healing, which could indicate how the pro- to anti-inflammatory phenotype switch is disrupted in type 2 diabetes (T2D), potentially leading to unresolved inflammation and disrupted wound repair.

The functional heterogeneity of macrophages has also been studied using the different functional markers they express. Matrix metalloproteinase-9 (MMP-9), a proinflammatory marker, degrades extracellular matrix (ECM) proteins and is essential for normal wound repair, but its increased expression is common in chronic wounds [13], especially in people with diabetes [14]. Our previous study found that high levels of MMP-9 in wound fluids were correlated with delayed wound healing in DFUs [15]. Adiponectin, a hormone secreted by adipose cells, can increase insulin sensitivity and decrease inflammation [16]. Lower levels of adiponectin and its receptors (AdipoR) have been found in people with obesity or T2D and in DFUs [16,17].

Although many of the studies mentioned above have highlighted the contributions of macrophage phenotypes and their functions to wound healing, it remains unclear how these phenotypes are represented in wounded skin tissues and how T2D dysregulate their function. Thus, it is necessary to study skin wound tissues in a preclinical model to understand the mechanisms and pathophysiology of wound healing.

A major limitation of current mouse models is that they often study only one sex in isolation, despite observed sex differences in immune responses, particularly in macrophage polarization [18]. Male sex is a well-reported prognostic factor for delayed wound healing, especially in venous leg ulcers and DFUs [19]. There is much evidence that sex may influence skin wound healing due to the effects of sex hormones and inherent differences in skin structure [20]. For example, estrogen deficiency in postmenopausal women contributes to delayed wound healing [21], whereas topical estrogen treatment accelerates healing in estrogendeficient female mice with T2D [22]. Additionally, men with diabetes are 1.5 times more likely to develop DFUs than women [23], and the severity of DFUs is greater in men, who are more likely to experience deeper and infected ulcers, critical limb ischemia, systemic infections and amputations [24,25]. However, even if sex-based physiological differences in wound healing exist, they could be influenced by behavioral and social differences. For example, women could be more likely to follow pressure-offloading medical advice and seek medical treatment more frequently [26,27].

Despite evidence of sex differences in skin wound healing, whether these differences exist in the phenotype and behavior of macrophages, in the presence or absence of T2D, has not yet been examined. This study aimed to investigate macrophage profiles in wounded skin tissues using a novel two-sex T2D mouse model. It was hypothesized that an imbalance between pro- and anti-inflammatory macrophage phenotypes in skin tissue would influence wound healing in T2D, to which sex differences also contribute.

2. Materials and Methods

2.1 Animal Model

Male (n = 14) and female (n = 14) C57BL/6J mice at 6 weeks old (Animal Resources Centre, Western Australia, Australia) were used in this study and randomly allocated into either the diabetes or control group. Diabetes was induced using a modified method from our previous study [28]. Briefly, the diabetes group (FaD: male n = 8; female n = 8) was fed an in-house high-fat diet containing 45% of calories from fat throughout the study period. After 8 weeks, the mice received intraperitoneal injections of streptozotocin (STZ; Calbiochem, San Diego, CA, USA) at 65 mg/kg of body weight. Male (n = 6) and female (n = 6) mice fed a chow diet containing 12% of calories from fat (Specialty Feeds, Glen Forrest, Western Australia, Australia) were included as controls (Chow). The mice were weighted weekly, and their random blood glucose level (BGL) was measured consistently in the morning.

After 18 weeks, each mouse received four circular full-thickness dorsal skin wounds, each 4mm in diameter, created using a punch biopsy. Surgery was performed under inhalational anesthesia with 5% isoflurane in 100% oxygen (flow rate: 1 L/min), maintained at 1–3% isoflurane. Each animal received opioid analgesia with buprenorphine (Temgesic, Sigma-Aldrich, St. Louis, MO, USA) at a dosage of 0.1 mg/kg body weight subcutaneously, administered prior to surgery and post-surgery for pain management.

At the time of wounding (Day 0), three wounded skin tissues from each mouse were collected for cytometry by time of flight (CyTOF) analysis [29]. At 10 days postwounding (Day 10), the male (Chow n = 5; FaD n = 8) and female (Chow n = 6; FaD n = 8) mice were euthanized under inhalational anesthesia with isoflurane in 100% oxygen (flow rate: 1 L/min), initially at 5% (v/v) for induction and maintained at 1–3% (v/v) to ensure deep anesthesia, followed by exsanguination via cardiac puncture. Two 8×8 mm square patches of skin surrounding their wounds were obtained per mouse for CyTOF analysis. One male Chow mouse was euthanized early at 4 days post-wounding due to wound infection.

The wound area was independently assessed by a blinded and an unblinded assessor, who digitally analyzed the photos taken at Day 0 and Day 10 post-wounding using ImageJ (v.2.1.0/1.53c, National Institutes of Health,



Bethesda, MD, USA). Two distinct methods were used to trace the open wound area: based on the wound outline, and the area that had not yet re-epithelialized [30]. The wound closure rate (WCR) was calculated and expressed as a percentage of the initial wound area that had closed by Day 10 post-wounding, recorded as WCR-O and WCR-E respectively [30]. Representative wound images are included in **Supplementary Fig. 1A**.

This study was approved by the University of Sydney Animal Ethics Committee (Project No.: 2020/1799) and carried out in accordance with the Australian Code for the Care and Use of Animals for Scientific Purposes 8th Edition 2013.

2.2 Preparation of Cell Suspension from Skin Tissues

Macrophage profiles of the collected skin tissues were analyzed by CyTOF, where antibodies were conjugated to Lanthanide heavy metals to detect intracellular and extracellular markers [31]. The freshly collected skin tissues at Day 0 and Day 10 were manually cut into smaller pieces, then incubated with Dispase II and Collagenase D (Sigma-Aldrich, St. Louis, MO, USA) [32,33]. To obtain a sufficient total cell count of 500,000 for CyTOF, samples were counted with Trypan Blue Solution (0.4%, Sigma-Aldrich, St. Louis, MO, USA) and pooled or diluted in fluorescence-activated cell sorting (FACS) buffer (0.5% BSA, 0.1% NaN3, 2 mM EDTA, in PBS; Sigma-Aldrich, St. Louis, MO, USA). The three skin wound samples from each mouse at Day 0 were pooled with those from mice of the same sex and diabetic status. The two square skin samples collected at Day 10 were pooled for each mouse.

2.3 Preparation for CyTOF

After washing in PBS, each sample was incubated with cisplatin (Cell-IDTM Cisplatin, Standard BioTools, South San Francisco, CA, USA), to exclude the dead cells, then with the antibody cocktail against cell surface antigens for 30 min on wet ice. Subsequently, the samples were washed in FACS buffer then incubated with Intracellular Fixation Buffer, permeabilized with Permeabilization Buffer (eBioscience™ Intracellular Fixation & Permeabilization Buffer Set, Thermo Fisher Scientific, Waltham, MA, USA), and incubated with the intracellular antibody for MMP-9 (Mouse MMP-9 Affinity Purified Polyclonal Antibody, R&D Systems, Minneapolis, MN, USA). The antibodies were prepared by the Ramaciotti Facility for Human Systems Biology (The University of Sydney, Sydney, NSW, Australia) and are described in **Supplementary Ta**ble 1. After washing with Permeabilization Buffer, DNA intercalator in paraformaldehyde was added. The samples were stored at 4 °C until the day of data acquisition.

On the day of acquisition, the cells were resuspended in Maxpar® Cell Acquisition Solution (CAS) (Standard BioTools, South San Francisco, CA, USA) for cell counting, then in a solution of EqTM Four Element Calibration

Beads (Standard BioTools, South San Francisco, CA, USA) and diluted 1:10 in CAS. Samples were processed in a Helios™ Mass Cytometer (Standard BioTools, South San Francisco, CA, USA), where 150,000–500,000 events were captured per sample and converted to flow cytometry standard (FCS) files.

2.4 Manual Gating of Macrophage Phenotypes

Using canonical cell surface markers for major cell subsets, a manual gating strategy was designed and implemented on the FCS files using FlowJo software (v.10.8.0, FlowJo LLC, Ashland, OR, USA). Calibration beads, nonsinglet cells, dead cells, granulocytes, eosinophils, B and T cells, natural killer cells, dendritic cells and monocytes were excluded. Total macrophages (F4/80+) and their main subsets were examined, including resident Langerhans cells (CD207+), infiltrating M1 and M2 macrophages and their subsets, and Ly6C+ and Ly6C- macrophages. The expression of functional markers AdipoR1 and MMP-9 by the macrophages and their subsets was also investigated. An example of the manual gating strategy used for Ly6C+ macrophages is displayed in Supplementary Fig. 2. To ensure accurate identification of cell populations, antibodies were titrated, and smoothing was applied to distinguish between positive and negative populations, with gates drawn on plots displaying individual cells.

Cell counts were recorded, and cell frequencies of the macrophage subsets were expressed as a proportion of the parent's population and analyzed for significant differences between mice of different sex and diabetic status. Within AdipoR1+ and MMP-9+ subsets, median signal intensity (MSI) of these functional markers was also measured and compared between groups.

2.5 Computational Analysis of Macrophage Phenotypes

To capture unique and unexpected macrophage populations missed by manual gating, computation analysis was performed using an R package, Spectre (v.0.4.7) [34]. Spectre utilizes mathematical modelling to identify clusters of cells expressing the same markers across all samples and allows the quantification of these clusters.

All samples were manually gated to macrophages (F4/80+), and the total frequencies of F4/80+ macrophages and their expression of subset markers were exported as comma-separated channel values for clustering. Using Spectre's FlowSOM algorithm, six metaclusters were generated around the six phenotypic clustering markers used in the manual gating strategy to gate for F4/80+ macrophage subsets: CD207, CD80, CD86, CD206, CD163 and Ly6C.

To visualize the data in two dimensions, dimensionality reduction was performed with the Uniform Manifold Approximation and Projection (UMAP) algorithm. The metaclusters were then annotated based on their high or low expression of certain markers. The proportions of these metaclusters were statistically analyzed to identify novel



macrophage subsets, their differential expression of phenotypic and functional markers, and any significant differences between groups.

To confirm and quantify the presence of metaclusters with significantly different proportions across groups, the manual gating strategy was further developed according to the metaclusters' profiles and applied to the F4/80+ macrophages in each manually gated sample using FlowJo. The proportions of these metaclusters were statistically analyzed and compared with Spectre's findings, to verify if novel macrophage subsets differed in proportion by sex or diabetic status.

2.6 Measurement of C-Peptide

C-peptide levels were measured in duplicate from plasma collected at Day 10 post-wounding using the Mouse C-Peptide ELISA kit (Crystal Chem, Chicago, IL, USA), following the manufacturer's protocol.

2.7 Statistical Analysis

All statistical tests were conducted using GraphPad Prism 9 software (v.9.0.2, Dotmatics, Boston, MA, USA). After assessing normality, two-tailed t-tests were performed for parametric data when comparing two groups (e.g., male vs female or FaD vs Chow), while two-way analysis of variance (ANOVA) was used for comparisons involving four groups (male FaD, male Chow, female FaD, and female Chow). The Tukey multiple comparisons test was used, with adjustment for multiple comparisons and an alpha level of 0.05. Non-parametric tests were employed for non-parametric data. Statistical significance was accepted at p < 0.05, with data presented as mean \pm standard error (SEM) for parametric data or as median with interquartile range for non-parametric data.

3. Results

3.1 Animal Characteristics

Although the mice were randomly allocated into four groups at the beginning of the experiment, the BGL of male FaD mice was slightly higher but still within the normal range at Week 0 compared to female FaD (p < 0.01). However, this difference was not significant at Week 4 (Fig. 1A). After 8 weeks of high-fat diet feeding (Week 8) and post-STZ injections (Week 9 onwards), male FaD mice had significantly higher BGL than female FaD (p < 0.05). The BGL of male and female Chow mice did not significantly differ except at Week 8, where male Chow had slightly higher BGL than female Chow (10.4 \pm 0.3 mmol/L vs 7.7 \pm 0.5 mmol/L, p < 0.05). Post-STZ injections, male FaD exhibited significantly higher BGL than male Chow (p <0.01). This trend was also observed in female FaD compared to Chow, but it only met statistical significance post-STZ at Week 13 (15.1 \pm 1.1 mmol/L vs 8.9 \pm 0.4 mmol/L) and pre-wounding at Week 18 (13.4 \pm 0.6 mmol/L vs 8.4 \pm 0.4 mmol/L) (both *p* < 0.05).

Throughout the study, male FaD and Chow mice were significantly heavier than female FaD and Chow mice respectively (p < 0.05) (Fig. 1B). After high-fat diet feeding and before STZ injections at Weeks 6–8, FaD mice were generally heavier than Chow mice, but this was only statistically significant for male FaD mice compared to Chow (p < 0.05).

At Day 10 post-wounding, male FaD mice had significantly higher C-peptide levels compared to both male Chow and female FaD mice (both p < 0.05) (Fig. 1C). Male Chow mice exhibited lower WCR-O than male FaD (61.5 \pm 9.8% vs 91.7 \pm 1.4%) and female Chow (61.5 \pm 9.8% vs 89.7 \pm 6.9%) (both p < 0.05) (Supplementary Fig. 1B). However, WCR-E was similar across all four groups, exceeding 96%, with no significant differences observed (Supplementary Fig. 1C).

3.2 Macrophage Profiles in Skin Tissue by Manual Gating

After excluding other types of immune cells such as granulocytes, eosinophils, B and T cells, natural killer cells, dendritic cells, and monocytes (**Supplementary Fig. 2**), total macrophages (F4/80+) were identified and expressed as a proportion of white blood cells (CD45+). Resident Langerhans cells, Ly6C+ and Ly6C- macrophages were gated under the F4/80+ macrophage population and expressed as a proportion of total macrophages. M1 and M2 macrophages and M2 subsets were further investigated under macrophages in the dermis (CD207-) and expressed as a proportion of these macrophages.

3.2.1 Total Macrophages (F4/80+)

Male mice had a greater proportion of total macrophages than females, significant only at Day 10 [male: 2.5% (1.8–3.1) vs female: 1.3% (1.2–1.8), p < 0.01] (Fig. 2A). However, the proportion of total macrophages did not differ significantly between the four groups at either Day 0 or Day 10.

As shown in Fig. 2A, at Day 0, there was a greater proportion of AdipoR1+ cells in F4/80+ macrophages in male FaD mice (60.8 \pm 16.5%) than in females (24.2 \pm 2.7%) (p < 0.05). This trend was reversed by Day 10, as the proportion of AdipoR1+ macrophages increased in female FaD mice and decreased in male FaD from Day 0, becoming significantly higher in female FaD mice (50.1 \pm 3.3%) than in males (40.8 \pm 2.1%) (p < 0.05). Additionally, at Day 10, the AdipoR1+ population in female FaD had a greater MSI (10.4 \pm 1.6) than in male FaD (6.0 \pm 0.8), a trend also seen in female Chow (11.24 \pm 1.1) compared to males (5.8 \pm 0.6) (p < 0.05).

At both Day 0 and Day 10, the majority of F4/80+ macrophages expressed MMP-9 (>70%) (Fig. 2A). At Day 0, the proportion of MMP-9+ F4/80+ macrophages did not show any differences between groups. However, at Day 10, there was a greater proportion of MMP-9+F4/80+ cells in male FaD (87.3 \pm 1.5%) than in females (73.1 \pm 2.1%)



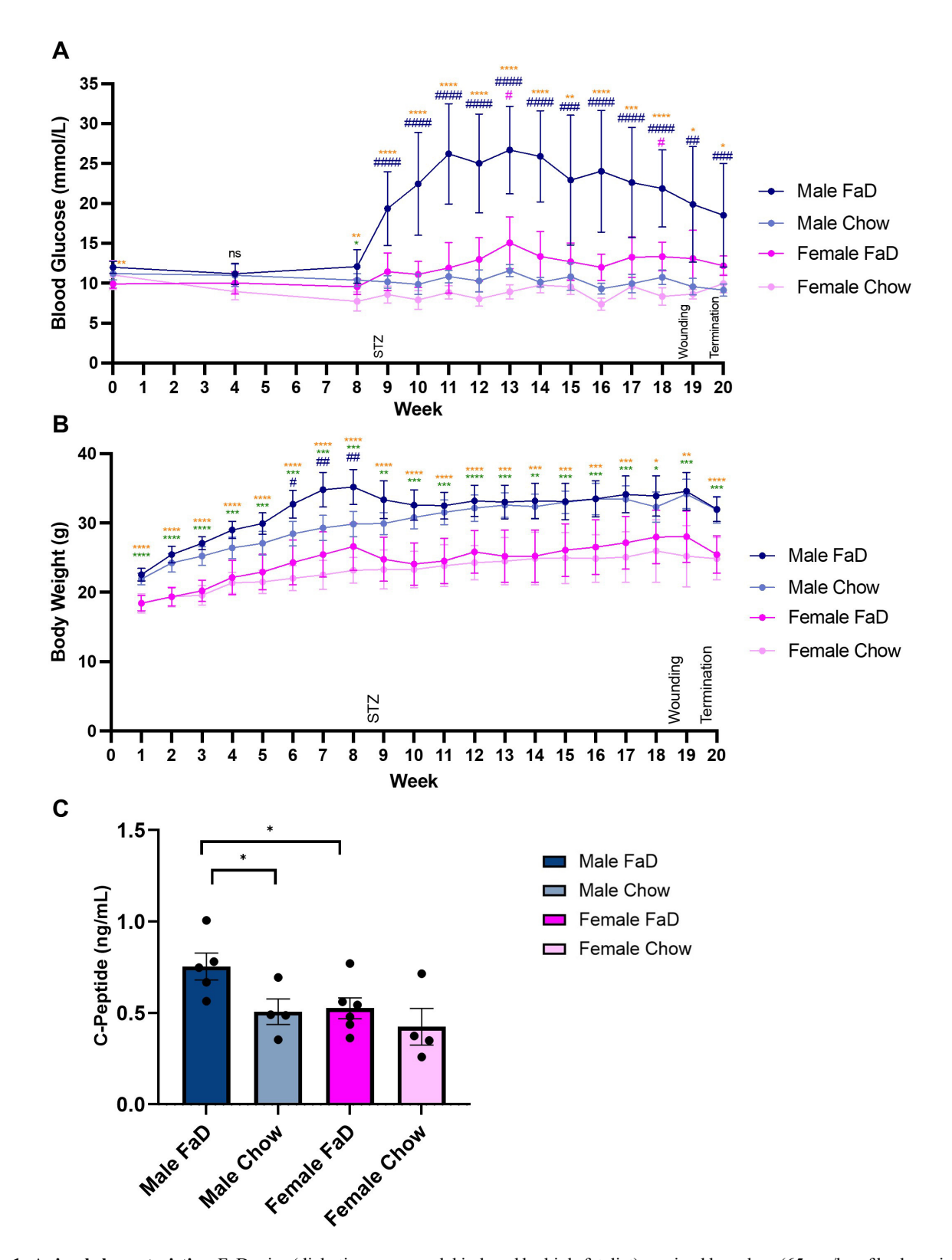


Fig. 1. Animal characteristics. FaD mice (diabetic mouse model induced by high-fat diet) received low-dose (65 mg/kg of body weight) STZ injections at Week 9. Wounding occurred at Week 19 and termination at Week 20. (A) Random blood glucose level (BGL). (B) Weekly body weight. (C) C-peptide levels at termination. Two-way analysis of variance (ANOVA) was performed to compare male FaD (n = 8), male Chow (control chow-fed mice) (n = 6 at all time points, except at termination, n = 5), female FaD (n = 8), and female Chow (n = 6). Significance was indicated as follows: no significance (ns), p < 0.05 (* or #), p < 0.01 (** or ##), p < 0.001 (*** or ###), p < 0.001 (*** or ###). Significant differences between groups were indicated as follows: male vs female FaD (orange *), male vs female Chow (green *), male FaD vs Chow (blue #), female FaD vs Chow (pink #).

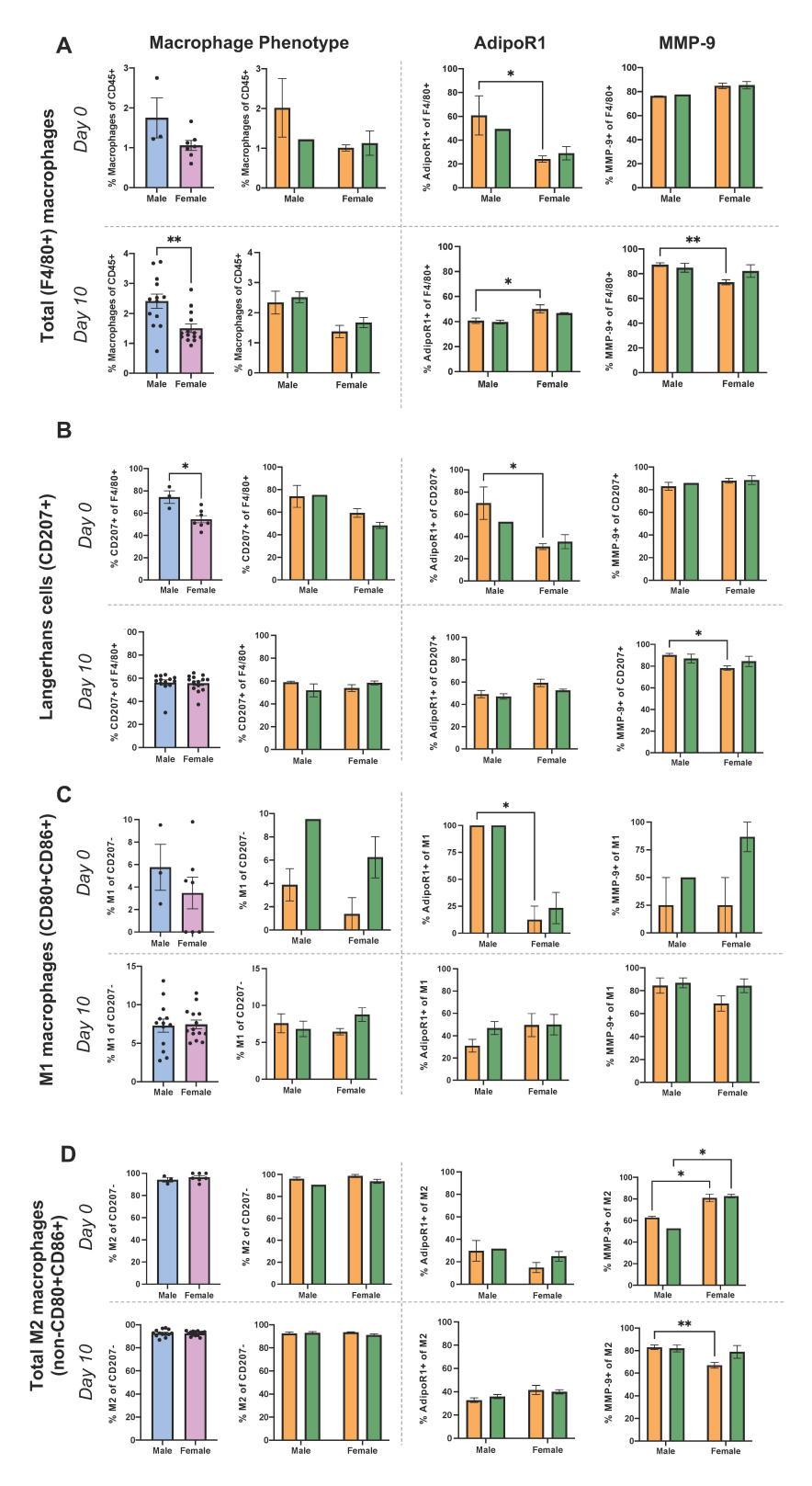


Fig. 2. Proportion of major macrophage subsets at Day 0 and Day 10 post-wounding. (A) Total (F4/80+) macrophages, (B) resident Langerhans cells (CD207+), (C) M1 (CD80+CD86+) and (D) total M2 (non-CD80+CD86+) macrophages were compared between male and female mice, or male FaD, male Chow, female FaD and female Chow mice. The proportion of macrophages expressing adiponectin receptor 1 (AdipoR1) or matrix metalloproteinase-9 (MMP-9) was also compared across the latter four groups. FaD groups are shown in orange, Chow in green. Day 0: male FaD (n = 2 samples), male Chow (n = 1 sample), female FaD (n = 4 samples), female Chow (n = 3 samples). Day 10: male FaD (n = 8 samples), male Chow (n = 5 samples), female FaD (n = 8 samples), female Chow (n = 6 samples). Significance was indicated as follows: p < 0.05 (*), p < 0.01 (**).

(p < 0.01). Additionally, although the lower proportion of MMP-9+F4/80+ macrophages in female FaD mice compared to Chow was not significant at Day 10, the MSI of MMP-9 in F4/80+ cells was significantly lower in female FaD mice (6.3 ± 0.6) than in Chow (12.9 ± 3.6) (p < 0.05).

3.2.2 Resident Langerhans Cells (CD207+)

As shown in Fig. 2B, at Day 0, male mice had a greater proportion of Langerhans cells (74.4 \pm 5.7%) than females (54.6 \pm 3.2%) (p < 0.05), but not Day 10. At both Day 0 and Day 10, the proportion of Langerhans cells did not differ significantly between the four groups.

The proportion of AdipoR1+ Langerhans cells was higher in male FaD (70.0 \pm 14.6%) than in females (30.9 \pm 2.7%) (p < 0.05), but only at Day 0.

The proportion of MMP-9+ Langerhans cells in all groups was generally high, especially at Day 0 (>80%). However, the only significant difference in this proportion was found at Day 10 between male FaD (90.2 \pm 1.4%) and female FaD mice (78.2 \pm 2.2%) (p < 0.05). Furthermore, the MSI of MMP-9 in MMP-9+ Langerhans cells was lower in female FaD (6.4 \pm 0.6) than in Chow (13.2 \pm 3.6) at Day 10 (p < 0.05).

3.2.3 M1 Macrophages (CD80+CD86+)

As shown in Fig. 2C, at Day 0 and Day 10, M1 macrophage proportion did not differ significantly between groups. At Day 0, all M1 macrophages in male mice had a greater proportion of AdipoR1+, and a significant difference was observed in male FaD mice (100.0 \pm 0.0%) compared to females (12.5 \pm 12.5%) (p < 0.05). However, by Day 10, the proportion of these macrophages decreased to below 50% in male FaD and Chow mice, without any significant differences.

The proportion of MMP-9+ M1 macrophages did not differ significantly between groups at Day 0 and Day 10. However, MMP-9 expression increased in male and female FaD groups at Day 10 (>60%) compared to Day 0 (<30%).

3.2.4 M2 Macrophages

3.2.4.1 Total M2 Macrophages (non-CD80+CD86+). Most of the macrophages present in the dermis (CD207-) were M2 macrophages at both Day 0 and Day 10 (>90%), although their proportion did not significantly differ between groups (Fig. 2D).

In addition, AdipoR1 expression by all groups was generally low, especially at Day 0 (<40%), and did not differ significantly between groups.

At Day 0, the proportion of MMP-9+ M2 macrophages was higher in female FaD mice (81.0 \pm 3.7%) than in males (62.7 \pm 1.2%) (p < 0.05), and in female Chow (82.6 \pm 1.6%) than in males (52.6%) (p < 0.05) (Fig. 2D). However, the opposite trend was present at Day 10; there was a greater proportion of MMP-9+ M2 macrophages in male FaD (82.9 \pm 2.1%) than in females

(67.0 \pm 2.5%) (p < 0.01). This proportion also increased in both male FaD and Chow groups from Day 0 (<65%) to Day 10 (>80%). The MSI of MMP-9 in MMP-9+ M2 macrophages was higher in female Chow (8.1 \pm 0.7) than in male Chow (2.4) at Day 0.

3.2.4.2 M2a Macrophages (CD206+CD163–). As shown in Fig. 3A, at Day 0, male mice had a greater proportion of M2a macrophages (21.7 \pm 3.4%) than females (9.1 \pm 2.6%) (p < 0.05), but not at Day 10.

AdipoR1 expression by M2a macrophages in all groups was generally low, especially at Day 0 (<40%), and did not differ significantly between groups at Day 0 and Day 10.

At Day 0, the proportion of MMP-9+ M2a macrophages was not significantly different between groups. However, at Day 10, this proportion was higher in male FaD mice (85.9 \pm 4.1%) than in females (68.1 \pm 3.8%) (p < 0.05).

3.2.4.3 M2b Macrophages (CD80–CD86+). As shown in Fig. 3B, most of the macrophages present in the dermis (CD207–) were specifically M2b macrophages (>60%) at both Day 0 and Day 10, and their proportion did not differ significantly between groups.

AdipoR1 expression by M2b macrophages in all groups was generally low (<45%) and did not significantly differ between groups.

At Day 0, the proportion of MMP-9+ M2b macrophages was higher in female FaD (84.3 \pm 2.6%) than in males (60.6 \pm 4.6%), and in female Chow (89.7 \pm 1.7%) than in males (50%, n = 1) (all p < 0.01). At Day 10, this trend was reversed; male FaD had a greater proportion of MMP-9+ M2b macrophages (84.8 \pm 2.2%) than females (67.3 \pm 2.1%) (p < 0.01). Additionally, this proportion was lower in female FaD mice (67.3 \pm 2.1%) compared to Chow (80.2 \pm 5.3%) (p < 0.05). The proportion of these macrophages in male FaD and Chow mice increased from Day 0 (<60%) to Day 10 (>80%).

3.2.4.4 M2c Macrophages (CD206+CD163+). As shown in Fig. 3C, the proportion of M2c macrophages did not differ significantly between groups at Day 0 and 10. However, their proportion in both male and female mice increased from Day 0 (<15%) to Day 10 (>30%).

AdipoR1 expression by M2c macrophages did not differ between groups. However, male FaD mice had a greater proportion of MMP-9+ M2c macrophages (84.6 \pm 1.6%) than females (67.6 \pm 2.9%) (p < 0.01), but only at Day 10. Additionally, this proportion was lower in female FaD (67.6 \pm 2.9%) than in Chow (83.4 \pm 6.3%) (p < 0.05) at Day 10.



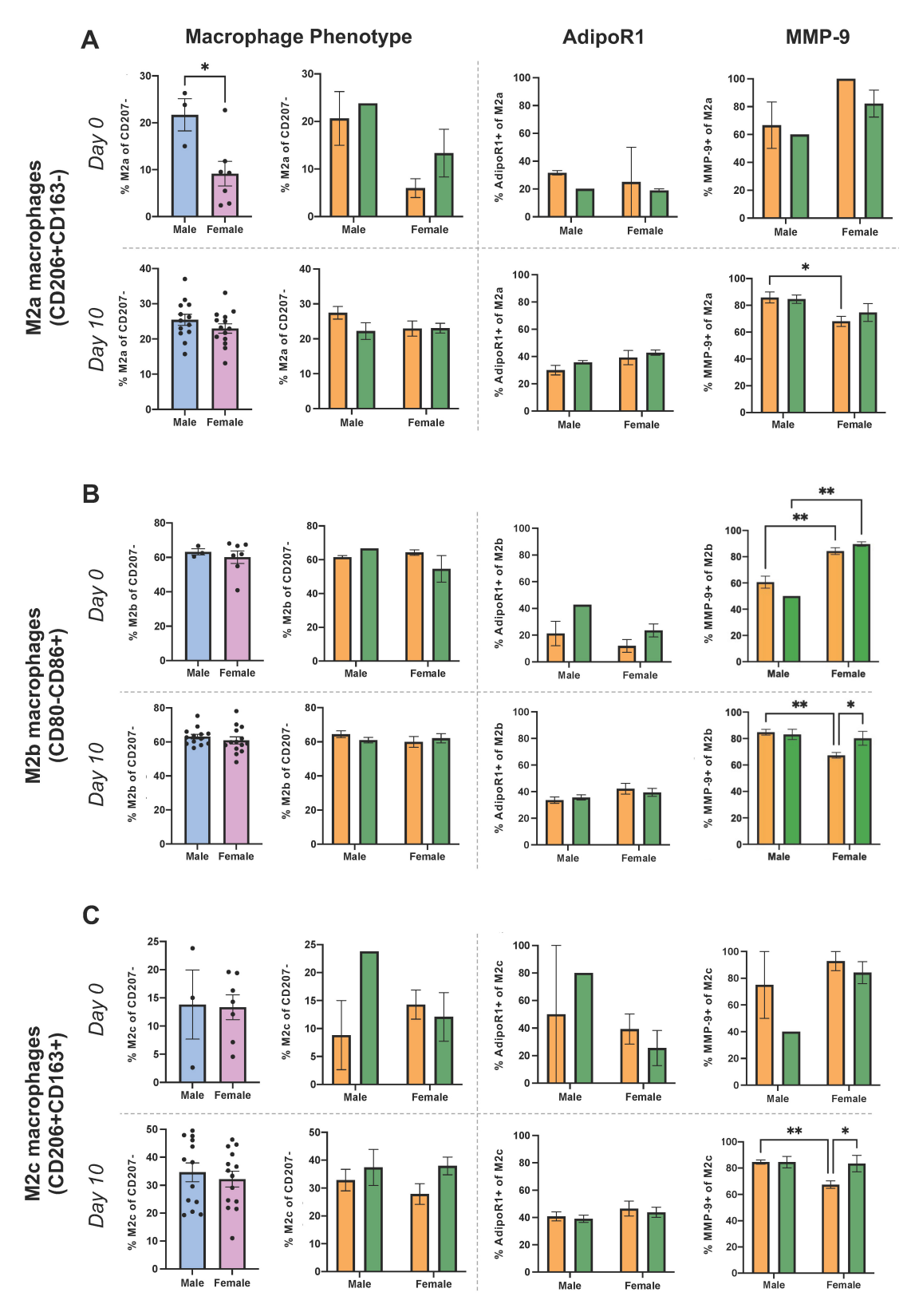


Fig. 3. Proportion of M2 macrophage subsets at Day 0 and Day 10 post-wounding. (A) M2a (CD206+CD163-), (B) M2b (CD80-CD86+) and (C) M2c (CD206+CD163+) macrophages were compared between male and female mice, or male FaD, male Chow, female FaD and female Chow mice. The proportion of macrophages expressing AdipoR1 or MMP-9 was also compared across the latter four groups. FaD groups are shown in orange, Chow in green. Day 0: male FaD (n = 2 samples), male Chow (n = 1 sample), female FaD (n = 4 samples), female Chow (n = 3 samples). Day 10: male FaD (n = 8 samples), male Chow (n = 5 samples), female FaD (n = 8 samples), female Chow (n = 6 samples). Significance was indicated as follows: p < 0.05 (*), p < 0.01 (**).

3.2.5 Ly6C+ Macrophages

Ly6C, a marker expressed by murine monocytes and macrophages, was found in significantly lower proportions in male mice (17.1 \pm 1.8%) compared to females (24.8 \pm 2.0%) at Day 10 (p < 0.01, **Supplementary Fig. 3A**). Notably, there was no significant difference between males and females at Day 0, nor between the four groups.

At both Day 0 and Day 10, the proportion of AdipoR1+ cells within the Ly6C+ macrophage population was high across all four groups (>90%) but did not differ between groups.

MMP-9 expression by Ly6C+ macrophages was generally high across all groups, especially at Day 0 (>80%). However, the only significant difference in the proportion of MMP-9+ Ly6C+ cells was found in male FaD (89.9 \pm 2.1%) compared to female FaD (74.5 \pm 2.3%) (p< 0.05) at Day 10.

3.2.6 Ly6C- Macrophages

As shown in **Supplementary Fig. 3B**, Ly6C–macrophages accounted for 50–85% of all F4/80+macrophages at Day 0, but there were no significant differences between male and female mice or all four groups. Similarly, the majority of F4/80+ macrophages were Ly6C– macrophages at Day 10, and male mice had a greater proportion of these macrophages (82.9 \pm 1.8%) than females (75.2 \pm 2.0%) (p < 0.01), but their proportion did not significantly differ between the four groups.

At Day 0 and Day 10, the proportion of AdipoR1+Ly6C-macrophages was generally low (<40%) and did not significantly differ between groups.

MMP-9 expression by Ly6C– macrophages was generally high across all groups at Day 0 and Day 10 (>70%), but the proportion of MMP-9+ Ly6C– macrophages was significantly in male FaD (86.4 \pm 1.7%) than in females (72.0 \pm 2.3%) at Day 10 (p < 0.01). Within MMP-9+ Ly6C– macrophages, the MSI of their MMP-9 expression was lower in female FaD (6.4 \pm 0.6) than in Chow mice (13.8 \pm 4.0) at Day 10 (p < 0.05).

For all macrophage phenotypes analyzed above, there were no significant differences in the proportion of macrophages, their subsets, or AdipoR1 and MMP-9 expression between FaD and Chow overall (data not shown).

3.3 Computational Metacluster Analysis

Fig. 4A shows an annotated two-dimensional representation of the six Spectre-generated metaclusters. Their expression of phenotypic and functional (AdipoR1 and MMP-9) markers was examined using the multi-plot in **Supplementary Fig. 4** and summarized in **Supplementary Table 2**.

Statistical tests were performed to determine whether the proportion of each macrophage metacluster (expressed as a proportion of F4/80+ macrophages) differed significantly across male FaD, male Chow, female FaD, and fe-

male Chow groups. There were no statistically significant differences in the proportion of metaclusters 1 and 2 across the groups (data not shown). Additionally, the proportion of metaclusters 3, 5 and 6 did not significantly differ between combined-sex FaD and Chow groups (data not shown). Although significant differences in metacluster 6 proportion were observed at Day 0 (data not shown), they were not considered as significant due to the small sample sizes of the groups.

3.3.1 Metacluster 3 (CD163-CD16+CD64+CD206+)

At Day 0 and Day 10, the proportion of metacluster 3 macrophages did not differ significantly between groups. However, at Day 10, there was a greater proportion of these macrophages in male mice (20.0 \pm 1.5%) than in females (15.7 \pm 1.2%) (p < 0.05) (Fig. 4B).

3.3.2 Metacluster 4 (CD163+CD16+CD64+CD206+)

At Day 0, there was a greater proportion of metacluster 4 macrophages in female mice (13.9 \pm 2.4%) than in males (3.9 \pm 1.6%) (p < 0.01), but not at Day 10. At Day 0 and Day 10, this proportion did not differ between the four groups (Fig. 4C).

3.3.3 Metacluster 5 (Ly6C+AdipoR1+CD163-CD206-)

At Day 0, the proportion of metacluster 5 macrophages did not differ significantly between groups (Fig. 4D). However, at Day 10, there was a smaller proportion of these macrophages in male mice (14.8 \pm 1.8%) than females (24.2 \pm 2.1%) (p < 0.01). There was also a greater proportion of these macrophages in female FaD (26.0 \pm 3.0%) than in males (14.5 \pm 2.4%) (p < 0.05) at Day 10.

3.4 Manual Gating Strategy for Novel Metaclusters

Due to significant inter-group differences found in the proportion of metacluster 3, 4 and 5 macrophages, a new manual gating strategy was developed to identify these populations from F4/80+ manually gated macrophages. Fig. 5A shows the manual gating method used for these metaclusters. CD206 and CD64 were not included in this gating strategy because of the variable expression of these markers within the metaclusters. After applying the manual gating strategy for these novel metaclusters to all F4/80+ manually gated samples, statistical tests were conducted to determine whether the proportion of these metaclusters differed significantly across the four groups.

There were no statistically significant differences in the proportion of manually gated metaclusters 3 and 4 across the groups (data not shown). For metacluster 5, there was a greater proportion in female mice (14.7 \pm 1.5%) compared to males (9.3 \pm 1.3%) at Day 10 (p < 0.05) (Fig. 5B). Otherwise, the proportions did not differ significantly between groups.



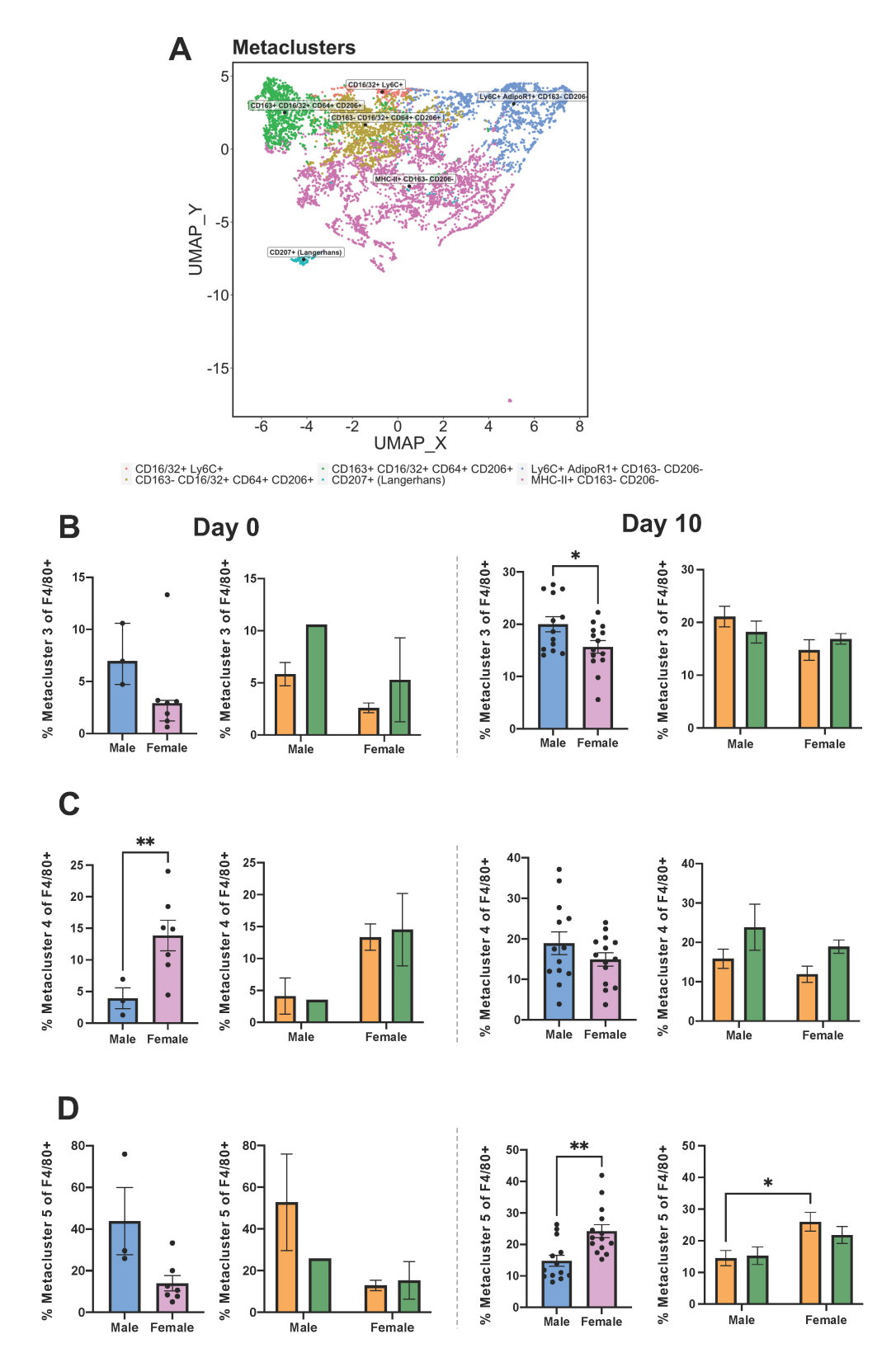


Fig. 4. Analysis of macrophage metaclusters identified by computational clustering. (A) Dimension-reduced UMAP plot of metaclusters. The proportion of (B) metacluster 3, (C) metacluster 4, and (D) metacluster 5 macrophages was compared between male and female mice, or male FaD, male Chow, female FaD and female Chow mice at Day 0 or Day 10 post-wounding. FaD groups are shown in orange, Chow in green. Day 0: male FaD (n = 2 samples), male Chow (n = 1 sample), female FaD (n = 4 samples), female Chow (n = 3 samples). Day 10: male FaD (n = 8 samples), male Chow (n = 5 samples), female FaD (n = 8 samples), female Chow (n = 6 samples). Significance was indicated as follows: p < 0.05 (*), p < 0.01 (**).

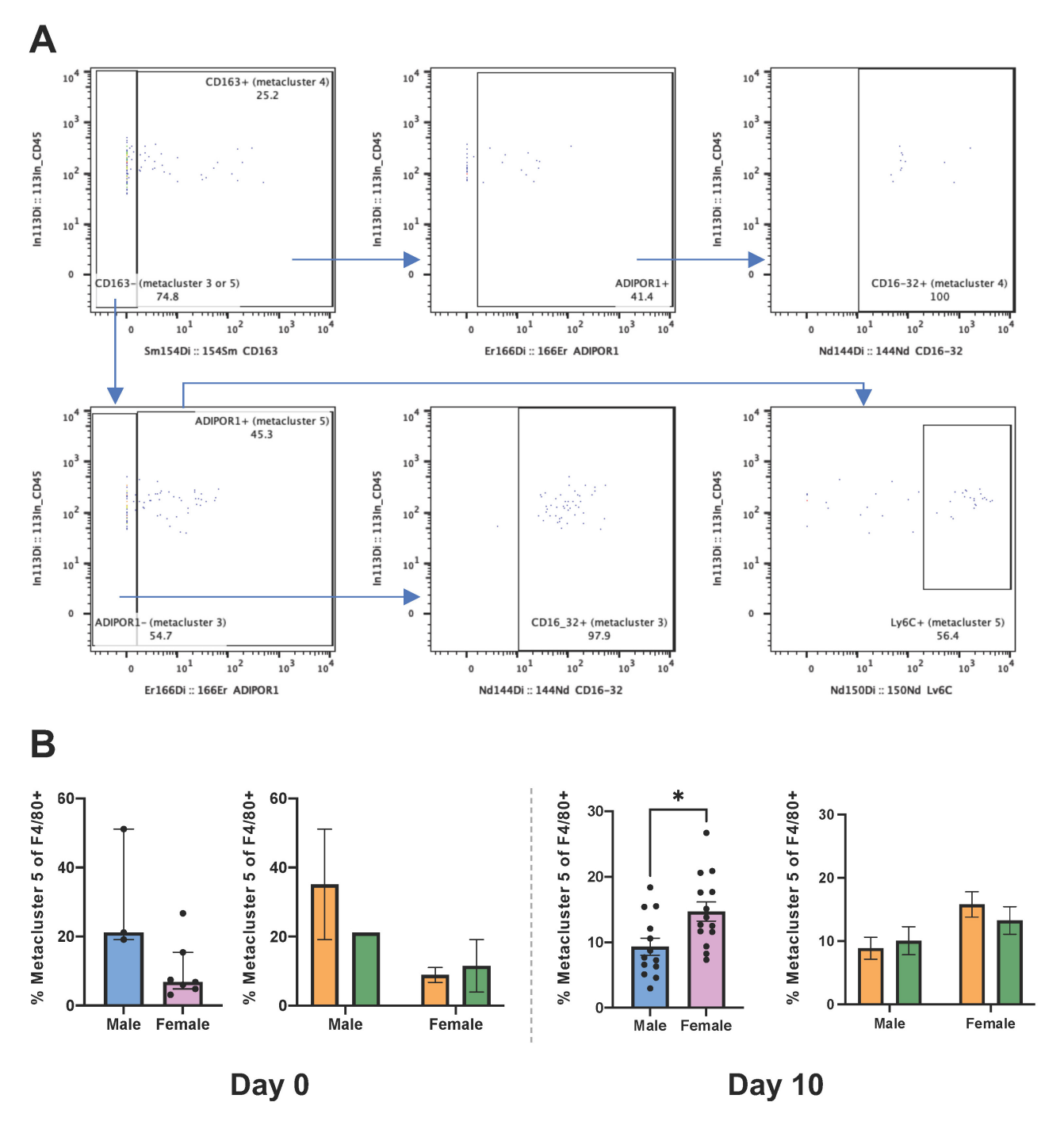


Fig. 5. Validation of novel macrophage metaclusters by manual gating. (A) Manual gating method for novel metaclusters, applied to F4/80+ manually gated macrophages. (B) The proportion of manually gated metacluster 5 (Ly6C+AdipoR1+CD163-) macrophages was compared between male and female mice, or male FaD, male Chow, female FaD and female Chow mice at Day 0 or Day 10 postwounding. FaD groups are shown in orange, Chow in green. Day 0: male FaD (n = 2 samples), male Chow (n = 1 sample), female FaD (n = 4 samples), female Chow (n = 3 samples). Day 10: male FaD (n = 8 samples), male Chow (n = 5 samples), female FaD (n = 8 samples), female Chow (n = 6 samples). Significance was indicated as p < 0.05 (*).

4. Discussion

Delayed wound healing is a common complication experienced by individuals with diabetes, particularly in the form of diabetic foot ulcers. These ulcers not only impose a significant health burden, but also create substantial economic challenges [1]. Chronic wounds typically arise from a complex interplay of factors, including excessive and prolonged inflammation [5], which is believed to be mediated by the accumulation of macrophages. How macrophage profiles are influenced by diabetes and sex during wound healing is unclear, which was investigated using CyTOF in



a diabetic mouse model in this study. We discovered distinct sex-based differences in pro- and anti-inflammatory macrophages and their expression of functional markers AdipoR1 and MMP-9 in skin wound tissue, suggesting that sex impacted skin macrophage phenotype and function during wound healing in diabetes.

In this study, male diabetic mice exhibited more severe hyperglycemia and insulin resistance than their female counterparts, which may be due to the regulatory effect of estrogen on glucose metabolism [35] and greater resistance to STZ in female mice [36]. The observed trend of male FaD mice having higher WCR-O than male Chow at Day 10, but no difference in WCR-E between groups, could be attributed to data loss. Several wounds could not be precisely digitally measured due to the regrowth of hair, which obscured accurate assessments. Nonetheless, further histological studies should be conducted to investigate pathological changes in wounded tissue and whether sex or diabetic status contributes to these.

Although there was no clear delayed wound healing observed in diabetic mice, we discovered several sex-based trends. Female Chow mice had significantly higher WCR-O than males at 10 days post-wounding, suggesting that sex had an influence on wound healing even in the absence of diabetes. This supports existing literature suggesting poorer wound healing in males than females [37–39]. One study of gonadectomized mice found that control nongonadectomized female mice had smaller wound areas than control males at 7 and 14 days post-wounding [37]. Indeed, androgenic hormones such as testosterone can inhibit skin wound healing in mice by encouraging inflammation [38], and androgen receptor knockout mice display accelerated wound healing [39], which could explain the poorer wound healing observed in the male Chow group in this study.

In addition, male mice had a significantly larger proportion of F4/80+ macrophages in the skin wound tissue than females at 10 days post-wounding. A recent study found a persistent accumulation of macrophages in wounded skin tissue of diabetic mice, which can enhance inflammation and prevent healing [16]. Similarly, in the gonadectomized mouse study, while male and female control mice exhibited impaired wound contraction and reepithelialization after exposure to chronic stress, there was an increase in F4/80+ macrophage numbers in male mice only [4]. Thus, our finding is consistent with the literature and suggests that an accumulation of macrophages in male mice could impair skin wound healing.

Furthermore, Ly6C- macrophages were the most abundant macrophage subset identified in skin wound tissue for both sexes at the time of wounding and 10 days post-wounding. A significantly higher proportion of this pro-resolutory subset and lower proportion of Ly6C+ macrophages was observed in male mice than female at 10 days post-wounding, suggesting that the wounds may still be in the proliferative phase of healing [17]. Thus,

in male mice, more macrophages are polarized towards an anti-inflammatory phenotype to promote healing at 10 days post-wounding, whereas this phase could have already passed in females, which could explain the higher WCR-O in female Chow compared to males at this timepoint.

MMP-9, a key player in regulating ECM degradation during wound healing [7], was also investigated in macrophages from skin wound tissue in this study. MMP-9 expression by total macrophages, Langerhans cells, Ly6C macrophages and M2 subsets was significantly higher in male FaD mice than females at Day 10 post-wounding, and this trend was observed in M1 macrophages without statistical significance. A recent study found upregulated MMP-9 expression in diabetic rat skin tissue and high glucose conditions in vitro [8]. Thus, the higher expression of MMP-9 in male FaD mice in our study may be partly attributed to more severe hyperglycemia. Although we did not find a direct association between MMP-9 expression and delayed wound healing in this study, our previous study and others have indicated that increased MMP-9 is associated with poor ulcer healing in people with diabetes [14,15], and inhibiting MMP-9 can accelerate diabetic wound healing while reducing inflammation [40].

Interestingly, at Day 0, there was a greater proportion of M2 macrophages expressing MMP-9 with a higher MSI in females than males, suggesting this phenotype may be in a more activated state. This relatively higher expression of MMP-9 mainly by M2b macrophages, which normally produce several other types of MMPs to aid their immunoregulatory functions [41], could enhance the regulation of wound healing in females. Further research is needed to fully understand the implications of these findings and their potential role in the wound healing process.

At 10 days post-wounding, MMP-9 was also highly expressed by M2b and M2c macrophages in Chow mice compared to FaD, but this pattern was observed only in female mice. Despite this, both female FaD and Chow mice achieved over 80% wound closure by Day 10 post-wounding. While M2b and M2c macrophages typically produce anti-inflammatory cytokines [42] and high levels of MMP-9 are associated with impaired wound healing [43], this suggests that the elevated MMP-9 in female Chow mice may have negatively affected their healing process, resulting in a wound closure rate similar to that of female FaD mice at 10 days post-wounding.

Adiponectin, an anti-inflammatory hormone, primarily acts on the AdipoR1 and AdipoR2 receptors, which are predominantly found in muscle tissue and the liver, respectively [16]. Additionally, adiponectin plays an important role in cutaneous wound healing [44,45]. Our study found that differences in AdipoR1 expression in macrophages are sex dependent. The proportion and expression of AdipoR1 in total macrophages were significantly lower in male FaD compared to females at 10 days post-wounding. However, this trend was reversed at the time of wounding, with



male FaD exhibiting a greater proportion of total and M1 macrophages as well as Langerhans cells expressing AdipoR1 than females. The decrease in AdipoR1 expression in these macrophage subsets from the time of wounding to 10 days post-wounding may contribute to poorer wound healing outcomes in males. A previous study showed that adiponectin deficiency is associated with impaired wound closure in mice, and topical adiponectin administration can improve wound healing in both adiponectin-deficient mice and diabetic mice [45].

To identify and quantify macrophage subsets and their expression of functional markers, this study used computational analysis techniques to complement traditional manual gating strategies. This blended approach allowed the identification and validation of novel macrophage subsets with unexpected marker combinations [46] that could be missed by a user-designed gating strategy [47], while ensuring they were still biologically relevant [30]. Metacluster 3 (CD163-CD16/32+CD64+CD206+) was a novel metacluster that was present in a higher proportion in male mice than females at 10 days post-wounding. It is likely an anti-inflammatory M2a-like subset (CD206+CD163-) with some pro-inflammatory functions, as CD64 and CD16/32 are markers for activated macrophages at sites of inflammation [48,49]. We also identified novel Metacluster 4 (CD163+CD16/32+CD64+CD206+), likely a similar M2clike subset with bacteria-induced local inflammatory functions (CD163+) [50]. There was a higher proportion of this metacluster in females than males at Day 0, which may be primarily beneficial to wound healing during the earlier inflammation phase and its transition into the proliferative phase [51].

Metacluster 5 (Ly6C+AdipoR1+CD163–CD206–) is likely a pro-inflammatory macrophage subset with pro-healing functions, as AdipoR1 is also involved in driving keratinocyte proliferation and migration for wound closure [52]. As Spectre and manual gating identified a significantly larger proportion of this metacluster in females than males at 10 days post-wounding, which was consistent with the higher AdipoR1 expression observed in female FaD than males at this timepoint, it could be a key driver of the observed delayed wound healing in male Chow mice and play an important role in the inflammatory to the proliferative stages of wound healing. Future studies could explore the cytokine expression and function of this macrophage phenotype in wound healing.

However, there are some limitations to our study design. Our novel two-sex diabetic mouse model requires further refinement to ensure that FaD mice display impaired wound healing. Alternative methods for diabetes induction in female mice should be considered, as female mice could be more resistant to high-fat diet-induced metabolic conditions [53]. For example, increasing the dosage of STZ to 75 mg/kg and administering it over five consecutive days could produce a more distinct diabetic pheno-

type in female mice [38]. Challenges with digitally assessing wound closure, such as capturing clear, valid images and judging re-epithelialization, must also be overcome. Also, future studies should include additional tissue collections at earlier endpoints to capture the full spectrum of macrophage phenotypic changes in different stages of wound healing [54,55]. It should be noted that sample sizes at Day 0 were relatively small, as some samples were pooled with others in the same group to achieve sufficient cell counts for CyTOF due to the small area of wounded skin. Moreover, future studies should incorporate cell count beads to standardize samples and report the absolute cell counts. Furthermore, the CyTOF panel should be modified to include markers for M2d macrophages, such as VEGF, IL-10, TGF- β and iNOS [56], and other markers to clearly separate resident dermal and infiltrating macrophages such as CX3CR1 [57]. Nonetheless, this study was still able to identify significant differences in macrophage polarization between male and female mice during wound healing in diabetes.

5. Conclusions

In conclusion, this study has uncovered previously unknown sex-related differences in skin macrophage phenotypes and their expression of functional markers. Male mice exhibited a greater proportion of total macrophages, particularly pro-inflammatory macrophages, as indicated by higher levels of MMP-9 and lower levels of AdipoR1 in male diabetic mice compared to females, suggesting a skewed polarization toward a pro-inflammatory phenotype in male diabetic mice that may contribute to poorer wound healing. Additionally, this study employed computational analysis and manual gating to identify a unique macrophage population (Ly6C+AdipoR1+CD163-CD206-) with a pro-inflammatory, pro-healing phenotype which was more abundant in females than males, suggesting its significant role in the transition from the inflammatory to the proliferative stages of wound healing. Overall, the combination of traditional and computational approaches in this study provides a more comprehensive understanding of the complexities of macrophage polarization during wound healing in diabetes. These insights can inform future explorations of leukocyte phenotypes and ultimately lead to the development of new therapeutic strategies to address impaired wound healing in diabetes.

Abbreviations

AdipoR, adiponectin receptor; ANOVA, analysis of variance; BGL, blood glucose level; CAS, cell acquisition solution; Chow, control chow-fed mice; CyTOF, cytometry by time of flight; Day 0, at the time of wounding; Day 10, at termination, 10-days post-wounding; DFUs, diabetes-related foot ulcers; ECM, extracellular matrix; FACS, fluorescence-activated cell sorting; FaD, diabetic mouse model induced by high-fat diet and STZ injection; MMP-9,



matrix metalloproteinase-9; MSI, median signal intensity; STZ, streptozotocin; T2D, type 2 diabetes; UMAP, uniform manifold approximation and projection; WCR, wound closure rate; WCR-E, wound closure rate measured by reepithelialization; WCR-O, wound closure rate measured by wound outline.

Availability of Data and Materials

The datasets generated and/or analyzed during the current study are available from the corresponding author upon reasonable request.

Author Contributions

CXH performed the experiment, data analysis and writing of the original manuscript draft; ES performed the animal work and assisted with data analysis; CJB assisted with computational metacluster analysis; ZW performed the ELISA experiment and data analysis; DS and HMM assisted with mass cytometry; SMT contributed to the animal model design and revision of the manuscript; DM contributed to the study design, supervision, and revision of the manuscript. All authors contributed to editorial changes in the manuscript. All authors have participated sufficiently in the work and agreed to be accountable for all aspects of the work. All authors read and approved the final manuscript.

Ethics Approval and Consent to Participate

This study was approved by the University of Sydney Animal Ethics Committee (Project No.: 2020/1799).

Acknowledgment

We thank members of Laboratory Animal Services (LAS) and Sydney Cytometry at the University of Sydney for their assistance in this project. We also thank Sarah L. Fox and Matilda Longfield from the Greg Brown Diabetes and Endocrine Research Laboratory for their assistance with the animal termination process. The graphical abstract was created with BioRender.

Funding

This work was supported by the Endocrinology Trust Fund from Royal Prince Alfred Hospital, Sydney, Australia. The funding source was not involved in the study design, collection and analysis of data, and preparation and submission of this article.

Conflict of Interest

The authors declare no conflict of interest.

Supplementary Material

Supplementary material associated with this article can be found, in the online version, at https://doi.org/10.31083/FBL27113.

References

- Jodheea-Jutton A, Hindocha S, Bhaw-Luximon A. Health economics of diabetic foot ulcer and recent trends to accelerate treatment. Foot. 2022; 52: 101909. https://doi.org/10.1016/j.foot.2022.101909.
- [2] Geraghty T, LaPorta G. Current health and economic burden of chronic diabetic osteomyelitis. Expert Review of Pharmacoeconomics & Outcomes Research. 2019; 19: 279–286. https: //doi.org/10.1080/14737167.2019.1567337.
- [3] Harding JL, Pavkov ME, Magliano DJ, Shaw JE, Gregg EW. Global trends in diabetes complications: a review of current evidence. Diabetologia. 2019; 62: 3–16. https://doi.org/10.1007/s00125-018-4711-2.
- [4] Sothornwit J, Srisawasdi G, Suwannakin A, Sriwijitkamol A. Decreased health-related quality of life in patients with diabetic foot problems. Diabetes, Metabolic Syndrome and Obesity: Targets and Therapy. 2018; 11: 35–43. https://doi.org/10.2147/DM SO.S154304.
- [5] Raziyeva K, Kim Y, Zharkinbekov Z, Kassymbek K, Jimi S, Saparov A. Immunology of Acute and Chronic Wound Healing. Biomolecules. 2021; 11: 700. https://doi.org/10.3390/biom 11050700.
- [6] Wang N, Liang H, Zen K. Molecular mechanisms that influence the macrophage m1-m2 polarization balance. Frontiers in Immunology. 2014; 5: 614. https://doi.org/10.3389/fimmu.2014. 00614.
- [7] Clayton K, Vallejo AF, Davies J, Sirvent S, Polak ME. Langer-hans Cells-Programmed by the Epidermis. Frontiers in Immunology. 2017; 8: 1676. https://doi.org/10.3389/fimmu.2017.01676.
- [8] Krzyszczyk P, Schloss R, Palmer A, Berthiaume F. The Role of Macrophages in Acute and Chronic Wound Healing and Interventions to Promote Pro-wound Healing Phenotypes. Frontiers in Physiology. 2018; 9: 419. https://doi.org/10.3389/fphys. 2018.00419.
- [9] Xu M, Chen Z, Chen K, Ma D, Chen L, DiPietro LA. Phagocytosis of apoptotic endothelial cells reprograms macrophages in skin wounds. Journal of Immunology and Regenerative Medicine. 2021; 12: 100038. https://doi.org/10.1016/j.regen. 2021.100038.
- [10] Wu X, He W, Mu X, Liu Y, Deng J, Liu Y, et al. Macrophage polarization in diabetic wound healing. Burns & Trauma. 2022; 10: tkac051. https://doi.org/10.1093/burnst/tkac051.
- [11] Geissmann F, Jung S, Littman DR. Blood monocytes consist of two principal subsets with distinct migratory properties. Immunity. 2003; 19: 71–82. https://doi.org/10.1016/s1074-7613(03) 00174-2.
- [12] Kimball A, Schaller M, Joshi A, Davis FM, denDekker A, Boniakowski A, et al. Ly6CHi Blood Monocyte/Macrophage Drive Chronic Inflammation and Impair Wound Healing in Diabetes Mellitus. Arteriosclerosis, Thrombosis, and Vascular Biology. 2018; 38: 1102–1114. https://doi.org/10.1161/ATVBAHA.118. 310703.
- [13] Kaur K, Singh A, Attri S, Malhotra D, Verma A, Bedi N, et al. Matrix metalloproteinases (MMPs) and diabetic foot: Pathophysiological findings and recent developments in their inhibitors of natural as well as synthetic origin. In Grimsby J, Derbel F (eds.) The Eye and Foot in Diabetes. IntechOpen: London, UK. 2020.
- [14] Nguyen TT, Ding D, Wolter WR, Pérez RL, Champion MM, Mahasenan KV, et al. Validation of Matrix Metalloproteinase-9 (MMP-9) as a Novel Target for Treatment of Diabetic Foot Ulcers in Humans and Discovery of a Potent and Selective Small-Molecule MMP-9 Inhibitor That Accelerates Healing. Journal of Medicinal Chemistry. 2018; 61: 8825–8837. https://doi.org/10.1021/acs.jmedchem.8b01005.



- [15] Liu Y, Min D, Bolton T, Nubé V, Twigg SM, Yue DK, et al. Increased matrix metalloproteinase-9 predicts poor wound healing in diabetic foot ulcers. Diabetes Care. 2009; 32: 117–119. https://doi.org/10.2337/dc08-0763.
- [16] Park HS, Lim JH, Kim MY, Kim Y, Hong YA, Choi SR, *et al.* Resveratrol increases AdipoR1 and AdipoR2 expression in type 2 diabetic nephropathy. Journal of Translational Medicine. 2016; 14: 176. https://doi.org/10.1186/s12967-016-0922-9.
- [17] Tuttolomondo A, La Placa S, Di Raimondo D, Bellia C, Caruso A, Lo Sasso B, *et al.* Adiponectin, resistin and IL-6 plasma levels in subjects with diabetic foot and possible correlations with clinical variables and cardiovascular co-morbidity. Cardiovascular Diabetology. 2010; 9: 50. https://doi.org/10.1186/1475-2840-9-50.
- [18] Dunn SE, Perry WA, Klein SL. Mechanisms and consequences of sex differences in immune responses. Nature Reviews. Nephrology. 2024; 20: 37–55. https://doi.org/10.1038/s41581-023-00787-w.
- [19] Marques R, Lopes M, Ramos P, Neves-Amado J, Alves P. Prognostic factors for delayed healing of complex wounds in adults: A scoping review. International Wound Journal. 2023; 20: 2869–2886. https://doi.org/10.1111/iwj.14128.
- [20] Thomason HA, Williams H, Hardman MJ. Klein SL, Roberts CW. Sex and Sex Hormones Mediate Wound Healing. Sex and Gender Differences in Infection and Treatments for Infectious Diseases (pp. 31–48). Springer International Publishing: Cham. 2015.
- [21] Horng HC, Chang WH, Yeh CC, Huang BS, Chang CP, Chen YJ, et al. Estrogen Effects on Wound Healing. International Journal of Molecular Sciences. 2017; 18: 2325. https://doi.org/10.3390/ ijms18112325.
- [22] Pincus DJ, Kassira N, Gombosh M, Berho M, Glassberg M, Karl M, et al. 17β-estradiol modifies diabetic wound healing by decreasing matrix metalloproteinase activity. Wounds. 2010; 22: 171–178.
- [23] McDermott K, Fang M, Boulton AJM, Selvin E, Hicks CW. Etiology, Epidemiology, and Disparities in the Burden of Diabetic Foot Ulcers. Diabetes Care. 2023; 46: 209–221. https://doi.org/10.2337/dci22-0043.
- [24] Vanherwegen AS, Lauwers P, Lavens A, Doggen K, Dirinck E, Initiative for Quality Improvement and Epidemiology in multidisciplinary Diabetic Foot Clinics (IQED-Foot) Study Group. Sex differences in diabetic foot ulcer severity and outcome in Belgium. PLoS ONE. 2023; 18: e0281886. https://doi.org/10. 1371/journal.pone.0281886.
- [25] Tang ZQ, Chen HL, Zhao FF. Gender differences of lower extremity amputation risk in patients with diabetic foot: a meta-analysis. The International Journal of Lower Extremity Wounds. 2014; 13: 197–204. https://doi.org/10.1177/ 1534734614545872.
- [26] Yazdanpanah L, Shahbazian H, Nazari I, Arti HR, Ahmadi F, Mohammadianinejad SE, et al. Incidence and Risk Factors of Diabetic Foot Ulcer: A Population-Based Diabetic Foot Cohort (ADFC Study)-Two-Year Follow-Up Study. International Journal of Endocrinology. 2018; 2018: 7631659. https://doi.org/10.1155/2018/7631659.
- [27] Sayiner ZA, Can FI, Akarsu E. Patients' clinical charecteristics and predictors for diabetic foot amputation. Primary Care Diabetes. 2019; 13: 247–251. https://doi.org/10.1016/j.pcd.2018. 12.002.
- [28] Lo L, McLennan SV, Williams PF, Bonner J, Chowdhury S, McCaughan GW, et al. Diabetes is a progression factor for hepatic fibrosis in a high fat fed mouse obesity model of nonalcoholic steatohepatitis. Journal of Hepatology. 2011; 55: 435– 444. https://doi.org/10.1016/j.jhep.2010.10.039.
- [29] Iyer A, Hamers AAJ, Pillai AB. CyTOF® for the Masses. Frontiers in Immunology. 2022; 13: 815828. https://doi.org/10.3389/

- fimmu.2022.815828.
- [30] Huang CX, Siwan E, Fox SL, Longfield M, Twigg SM, Min D. Comparison of digital and traditional skin wound closure assessment methods in mice. Laboratory Animal Research. 2023; 39: 25. https://doi.org/10.1186/s42826-023-00176-1.
- [31] Spitzer MH, Nolan GP. Mass Cytometry: Single Cells, Many Features. Cell. 2016; 165: 780–791. https://doi.org/10.1016/j.ce ll.2016.04.019.
- [32] Li Z, Gothard E, Coles MC, Ambler CA. Quantitative Methods for Measuring Repair Rates and Innate-Immune Cell Responses in Wounded Mouse Skin. Frontiers in Immunology. 2018; 9: 347. https://doi.org/10.3389/fimmu.2018.00347.
- [33] Shakya S, Asosingh K, Mack JA, Maytin EV. Optimized protocol for the preparation of single cells from cutaneous wounds for flow cytometric cell sorting and analysis of macrophages. MethodsX. 2020; 7: 101027. https://doi.org/10.1016/j.mex.2020.
- [34] Ashhurst TM, Marsh-Wakefield F, Putri GH, Spiteri AG, Shinko D, Read MN, et al. Integration, exploration, and analysis of high-dimensional single-cell cytometry data using Spectre. Cytometry. Part a. 2022; 101: 237–253. https://doi.org/10.1002/cyto.a. 24350.
- [35] Kim B, Kim YY, Nguyen PT-T, Nam H, Suh JG. Sex differences in glucose metabolism of streptozotocin-induced diabetes inbred mice (C57BL/6J). Applied Biological Chemistry. 2020; 63: 1–8.
- [36] Saadane A, Lessieur EM, Du Y, Liu H, Kern TS. Successful induction of diabetes in mice demonstrates no gender difference in development of early diabetic retinopathy. PLoS ONE. 2020; 15: e0238727. https://doi.org/10.1371/journal.pone.0238727.
- [37] Romana-Souza B, Assis de Brito TL, Pereira GR, Monte-Alto-Costa A. Gonadal hormones differently modulate cutaneous wound healing of chronically stressed mice. Brain, Behavior, and Immunity. 2014; 36: 101–110. https://doi.org/10.1016/j.bbi.2013.10.015.
- [38] Ashcroft GS, Mills SJ. Androgen receptor-mediated inhibition of cutaneous wound healing. The Journal of Clinical Investigation. 2002; 110: 615–624. https://doi.org/10.1172/JCI15704.
- [39] Lai JJ, Lai KP, Chuang KH, Chang P, Yu IC, Lin WJ, et al. Monocyte/macrophage androgen receptor suppresses cutaneous wound healing in mice by enhancing local TNF-alpha expression. The Journal of Clinical Investigation. 2009; 119: 3739– 3751. https://doi.org/10.1172/JCI39335.
- [40] Chen J, Qin S, Liu S, Zhong K, Jing Y, Wu X, et al. Targeting matrix metalloproteases in diabetic wound healing. Frontiers in Immunology. 2023; 14: 1089001. https://doi.org/10.3389/fimm u.2023.1089001.
- [41] Hesketh M, Sahin KB, West ZE, Murray RZ. Macrophage Phenotypes Regulate Scar Formation and Chronic Wound Healing. International Journal of Molecular Sciences. 2017; 18: 1545. https://doi.org/10.3390/ijms18071545.
- [42] Wang LX, Zhang SX, Wu HJ, Rong XL, Guo J. M2b macrophage polarization and its roles in diseases. Journal of Leukocyte Biology. 2019; 106: 345–358. https://doi.org/10.1002/JLB.3RU1018-378RR.
- [43] Sabino F, Auf dem Keller U. Matrix metalloproteinases in impaired wound healing. Metalloproteinases in Medicine. 2015; 2: 1–8.
- [44] Salathia NS, Shi J, Zhang J, Glynne RJ. An in vivo screen of secreted proteins identifies adiponectin as a regulator of murine cutaneous wound healing. The Journal of Investigative Dermatology. 2013; 133: 812–821. https://doi.org/10.1038/jid.2012.374.
- [45] Shibata S, Tada Y, Asano Y, Hau CS, Kato T, Saeki H, et al. Adiponectin regulates cutaneous wound healing by promoting keratinocyte proliferation and migration via the ERK signaling pathway. Journal of Immunology. 2012; 189: 3231–3241. https://doi.org/10.4049/jimmunol.1101739.



- [46] Marsh-Wakefield FM, Mitchell AJ, Norton SE, Ashhurst TM, Leman JK, Roberts JM, et al. Making the most of highdimensional cytometry data. Immunology and Cell Biology. 2021; 99: 680–696. https://doi.org/10.1111/imcb.12456.
- [47] Gondois-Rey F, Granjeaud S, Rouillier P, Rioualen C, Bidaut G, Olive D. Multi-parametric cytometry from a complex cellular sample: Improvements and limits of manual versus computational-based interactive analyses. Cytometry. Part A. 2016; 89: 480–490. https://doi.org/10.1002/cyto.a.22850.
- [48] Akinrinmade OA, Chetty S, Daramola AK, Islam MU, Thepen T, Barth S. CD64: An Attractive Immunotherapeutic Target for M1-type Macrophage Mediated Chronic Inflammatory Diseases. Biomedicines. 2017; 5: 56. https://doi.org/10.3390/biomedicines5030056.
- [49] Ong SM, Teng K, Newell E, Chen H, Chen J, Loy T, et al. A Novel, Five-Marker Alternative to CD16-CD14 Gating to Identify the Three Human Monocyte Subsets. Frontiers in Immunology. 2019; 10: 1761. https://doi.org/10.3389/fimmu. 2019.01761.
- [50] Fabriek BO, van Bruggen R, Deng DM, Ligtenberg AJM, Nazmi K, Schornagel K, et al. The macrophage scavenger receptor CD163 functions as an innate immune sensor for bacteria. Blood. 2009; 113: 887–892. https://doi.org/10.1182/bloo d-2008-07-167064.
- [51] Wilkinson HN, Hardman MJ. Wound healing: cellular mechanisms and pathological outcomes. Open Biology. 2020; 10: 200223. https://doi.org/10.1098/rsob.200223.

- [52] Oh J, Lee Y, Oh SW, Li T, Shin J, Park SH, et al. The Role of Adiponectin in the Skin. Biomolecules & Therapeutics. 2022; 30: 221–231. https://doi.org/10.4062/biomolther.2021.089.
- [53] Oraha J, Enriquez RF, Herzog H, Lee NJ. Sex-specific changes in metabolism during the transition from chow to high-fat diet feeding are abolished in response to dieting in C57BL/6J mice. International Journal of Obesity (2005). 2022; 46: 1749–1758. https://doi.org/10.1038/s41366-022-01174-4.
- [54] Masson-Meyers DS, Andrade TAM, Caetano GF, Guimaraes FR, Leite MN, Leite SN, et al. Experimental models and methods for cutaneous wound healing assessment. International Journal of Experimental Pathology. 2020; 101: 21–37. https://doi.org/10.1111/iep.12346.
- [55] Sharifiaghdam M, Shaabani E, Faridi-Majidi R, De Smedt SC, Braeckmans K, Fraire JC. Macrophages as a therapeutic target to promote diabetic wound healing. Molecular Therapy. 2022; 30: 2891–2908. https://doi.org/10.1016/j.ymthe.2022.07.016.
- [56] Heusinkveld M, van der Burg SH. Identification and manipulation of tumor associated macrophages in human cancers. Journal of Translational Medicine. 2011; 9: 216. https://doi.org/10. 1186/1479-5876-9-216.
- [57] Kolter J, Feuerstein R, Zeis P, Hagemeyer N, Paterson N, d'Errico P, et al. A Subset of Skin Macrophages Contributes to the Surveillance and Regeneration of Local Nerves. Immunity. 2019; 50: 1482–1497.e7. https://doi.org/10.1016/j.immuni .2019.05.009.

